Multimodality Cardiac Imaging Assessment of a Large Metastatic Pericardial Leiomyosarcoma

Apichaya Sripariwuth, MD, Bo Xu, MD, Huang Steve Shih-lin, MD, PhD, Ryan S. Berry, MD, Sudish Murthy, MD, PhD, Gosta Pettersson, MD, PhD, and Christine Jellis, MD, PhD,
Cleveland, Ohio

INTRODUCTION

Uterine leiomyosarcomas (ULMS) are rare tumors, with an incidence of 0.64 cases per 100,000 women.[1] The common sites of metastases are lung, peritoneum, and bone. Cardiac metastases are very rare. The reported sites of cardiac metastases mainly involve the right heart and associated structures. This is the first case report of a large pericardial metastatic leiomyosarcoma, with no associated lung metastasis. We illustrate how multimodality cardiovascular imaging was used for diagnosis and surgical planning.

CASE PRESENTATION

A 56-year-old woman was referred to our center for further investigation and management of a large pericardial mass. At presentation, she was clinically well. Her vital signs were stable (pulse rate 61 beats/min, regular; blood pressure 135/80 mm Hg). Her relevant history included total abdominal hysterectomy with bilateral salpingo-oophorectomy for a high-grade leiomyosarcoma (estrogen receptor–positive 20%, progesterone receptor–positive 100%, and human epidermal growth factor receptor 2/neu–negative) in August 2008. She had been maintained on anastrozole for 1.5 years before presentation. She did well until late 2016, when she developed shortness of breath, orthopnea, and lower extremity edema. Echocardiography showed bilateral pleural effusions, a large pericardial effusion with tamponade physiology, and a pericardial mass. She underwent urgent pericardial window, pericardial drainage, and pericardial biopsy. Histopathology from the pericardial biopsy demonstrated chronic inflammation with no malignancy seen, though sampling was limited. Subsequently, a localized mass was discovered in the patient's right submandibular gland. She underwent submandibular gland resection in March 2017. Histopathology demonstrated evidence of metastatic leiomyosarcoma.

Since that time, the patient has had progressive shortness of breath and palpitations, associated with weight loss. Positron emission tomography (PET) with ^{18}F-fluorodeoxyglucose (FDG) was performed and demonstrated mildly increased FDG uptake within the solid part of the large pericardial mass (Figure 1). There was an additional mildly FDG-avid paravertebral mass, with focal sternal FDG uptake, suggestive of metastatic disease. Chest and abdominal computed tomography (CT) also demonstrated a large lobulated, mixed solid-cystic pericardial mass (Figure 2A). There was a small region of possible myocardial invasion into the inferoposterior aspect of the left ventricle (Figure 2B). The left circumflex artery and its branches were "entrapped" and compressed between the mass and the left heart (Figure 3, Video 1).

Transthoracic echocardiography (TTE; Figure 4, Video 2) and TEE (Figure 5, Video 3) demonstrated a large heterogeneous mass lateral to the left ventricle. Additionally, there was a cystic component associated with the mass. There was no obvious invasion of the myocardium.

Cardiac magnetic resonance imaging (CMR) revealed a large mixed solid-cystic pericardial mass (Figures 6A–6C). The solid portion demonstrated heterogeneously hyperintense signal on black blood, white blood, and T2-weighted imaging and heterogeneous enhancement on perfusion imaging. The cystic portion demonstrated high signal intensity on T1-weighted and T2-weighted imaging without enhancement on perfusion imaging. There was uniform circumferential increased signal (suggesting fibrous encapsulation) around the lateral aspect of the mass, which was not as evident adjacent to the left ventricular lateral wall, where tissue planes were not well defined (Figure 6D). The overall features on CMR were supportive of a malignant tumor. Adherence to the anterolateral wall of the left ventricle, pericardium, and the lateral wall of the left atrium was also noted. No distinct invasion of the left ventricular myocardium was observed, although this could not be excluded, as tissue planes were not well defined. There was mild compression of the left atrium without obvious wall or chamber invasion. The mass measured approximately 12.0 × 7.0 cm in the axial plane and 9.5 × 8.7 cm in the sagittal plane (Figure 7).

Following multimodality cardiovascular imaging assessment, the pericardial mass was deemed resectable. At the time of the operation, the mass appeared to arise from a pedicle on the posterolateral aspect of the left ventricle, with a small amount of epicardial invasion into the posterolateral surface of the left ventricle (Figure 8). The mass was resected, with clear margins (Figure 9).

Histopathologic examination of the mass demonstrated a proliferation of elongated spindle cells with eosinophilic cytoplasm and

From the Department of Radiology (A.S., H.S.S.), the Department of Cardiovascular Medicine (B.X., C.J.), the Department of Pathology (R.S.B.), and the Department of Thoracic and Cardiovascular Surgery (S.M., G.P.), Heart and Vascular Institute, Cleveland Clinic, Cleveland, Ohio.

Keywords: Pericardial metastasis, Uterine leiomyosarcoma, Transesophageal echocardiography, Multidetector cardiac computed tomography, Cardiac magnetic resonance imaging

Conflicts of interest: The authors reported no actual or potential conflicts of interest relative to this document.

2468-6441

https://doi.org/10.1016/j.case.2018.04.007

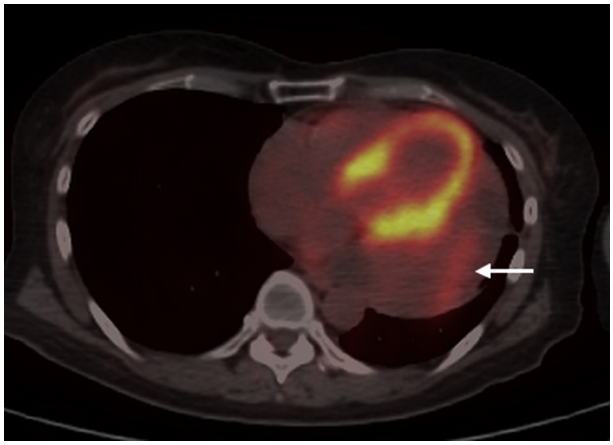

Figure 1 FDG PET/CT demonstrating radiotracer uptake in the solid part of the pericardial mass (*white arrow*). Maximum standardized uptake value is 3.48.

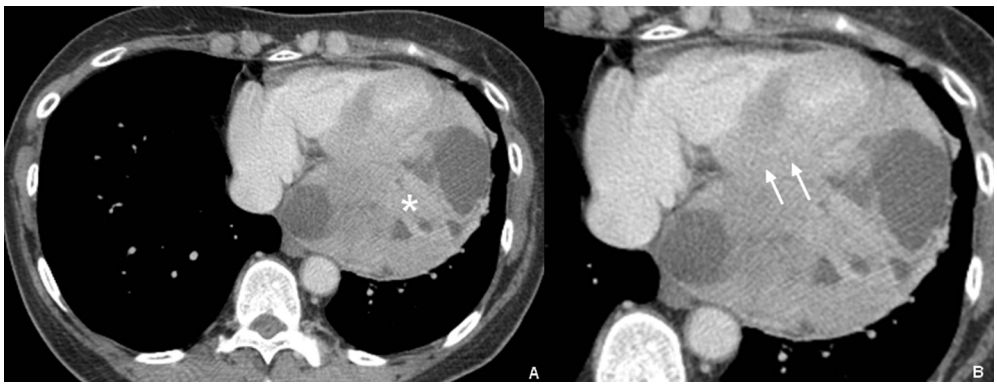

Figure 2 **(A)** Contrast-enhanced axial computed tomographic scan, demonstrating a large mixed solid-cystic pericardial mass. The solid component shows heterogeneous enhancement (*asterisk*). **(B)** Contrast-enhanced axial computed tomographic scan (zoomed-in image) demonstrating no distinction in the fat plane separating the mass from the myocardium at the inferoposterior aspect of the left ventricle (*white arrows*).

oblong blunt-ended nuclei arranged in intersecting fascicles (Figure 10A). Numerous mitotic figures were identified (14/10 high-power fields). Immunohistochemical stains were positive for smooth muscle actin and desmin (Figure 10B). Pathologic findings confirmed with metastatic pericardial leiomyosarcoma. Five days after surgery, the patient was discharged. This patient was last seen at our center when she came for postoperative FDG PET/CT (1 month after surgery). Postoperative FDG PET/CT at 1 month showed no definite residual FDG-avid disease in the resection bed. She is now followed up locally, and we do not have any further information.

DISCUSSION

Uterine sarcomas are rare neoplasms that can be classified into three types by composition: smooth muscle tumors, endometrial stromal tumors, and tumors with both smooth muscle and epithelial components.[2] Leiomyosarcoma is a malignant neoplasm with smooth muscle differentiation and the second most common subtype of uterine sarcoma.[2] In most cases, the diagnosis of ULMS is made following hysterectomy or myomectomy for presumed benign uterine leiomyomas. The standard management of a localized ULMS is surgical and includes total abdominal hysterectomy with or without salpingo-oophorectomy. In patients with extrauterine disease spread, additional surgical resection of metastatic disease or systemic chemotherapy is recommended, depending on the staging of the disease. ULMS is biologically aggressive and has a propensity for early hematogenous spread.[3] Local recurrence and metastatic disease predict poor outcomes. In a recent study of 113 patients, the most common sites of metastases from uterine sarcoma were lung (74%), peritoneum (41%), bone (33%), and liver (27%).[4] Metastasis to the heart is rare. The reported sites of cardiac metastases mainly involve the right heart and associated structures, particularly the right atrium and the

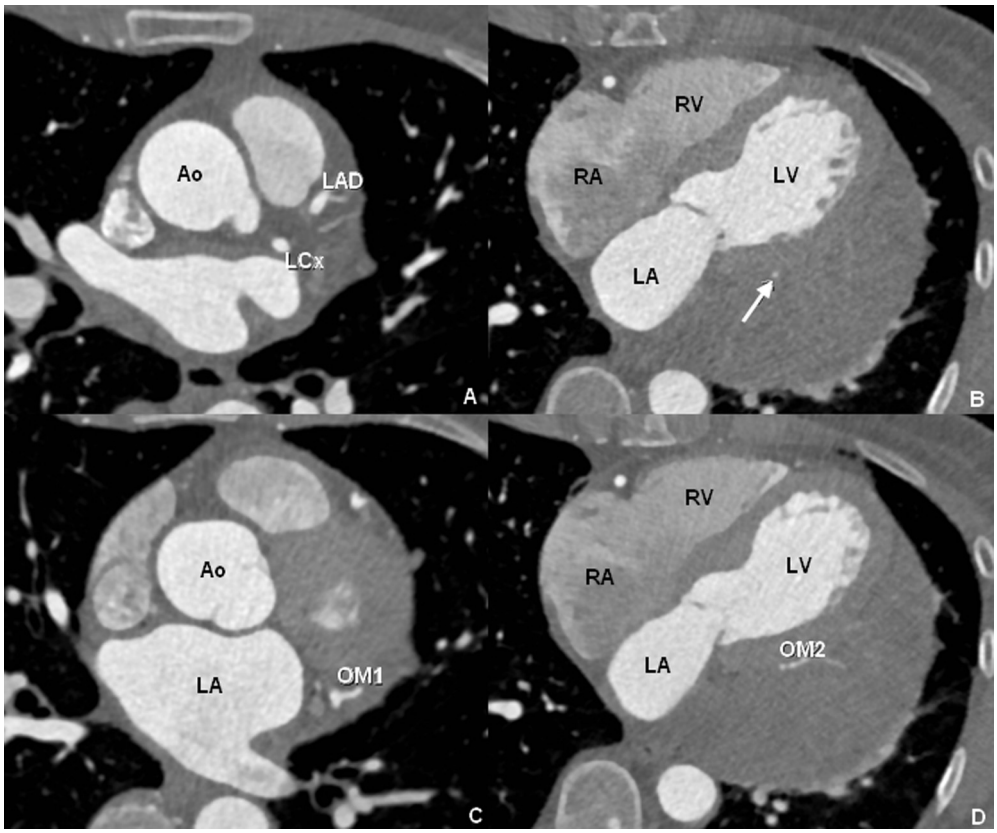

Figure 3 Coronary computed tomographic angiography, demonstrating that the left circumflex artery (LCx; **A**) and, in particular, the second obtuse marginal branch (OM2) of the LCx were entrapped and compressed (*arrow* in **B**; **D**) between the mass and left ventricle (LV). Note that in comparison, the first obtuse marginal branch (OM1; **C**) of the LCx did not appear to be compressed by the mass. *Ao*, Aorta; *LA*, left atrium; LAD, left anterior descending coronary artery; *RA*, right atrium; *RV*, right ventricle.

pulmonary artery.[5] There are 12 cases of cardiac metastases from ULMS in the English literature. Half were diagnosed by CT, when patients were investigated for suspected pulmonary embolism[6-9] and pulmonary nodules.[10,11] Four cases were diagnosed by echocardiography, and congestive heart failure was the most common presentation.[3,5,12] Prior case reports demonstrated that metastatic deposits can be found in various cardiac chambers and valves, but none reported pericardial metastatic involvement by leiomyosarcoma: three cases reported metastatic deposits in the left atrium,[3,5,6] two involving the right atrium,[7,8] two with right ventricular involvement,[11,13] two cases demonstrated left ventricular involvement,[12,14] and one report each demonstrating mitral[15] and tricuspid valve[9] involvement, respectively. In general, tumors may spread to the heart and pericardium by one of four pathways: (1) retrograde lymphatic extension, (2) hematogenous spread, (3) direct contiguous extension, and (4) transvenous extension. The parietal pericardium has a scant blood supply, and the visceral pericardium contains most of the lymphatic channels that drain the pericardial space. Therefore, the postulated metastatic pathway for pericardial metastasis in our patient may involve retrograde lymphatic extension and hematogenous spread.

One case detected cardiac metastasis as an incidental finding by CMR.[15] Only one previous patient had undergone PET/CT for primary tumor staging.[13] Our case is the first to demonstrate the utility of multimodality imaging for diagnostic purposes and for treatment guidance.

Our case of a large pericardial metastatic leiomyosarcoma with comprehensive multimodality cardiovascular imaging assessment is very rare. Early diagnosis of cardiac metastases may be difficult. Signs and symptoms are nonspecific and highly variable, related to the localization, size, and composition of the cardiac mass. Because of its low cost, portability, widespread availability, and lack of ionizing radiation, TTE remains the first-line imaging modality for the evaluation of a patient with a suspected cardiac mass. It allows localization of the mass and evaluation of other cardiac structures and function. TEE provides superior spatial resolution and better visualization of some cardiac masses than TTE,

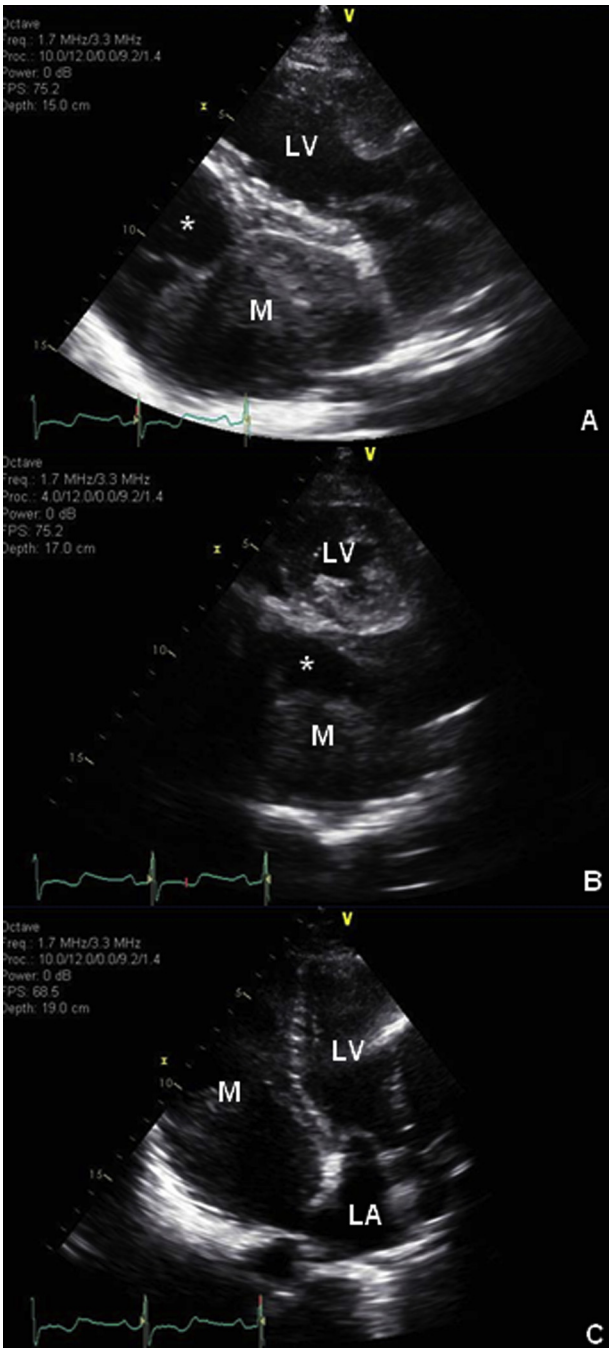

Figure 4 Transthoracic echocardiographic assessment of the pericardial mass. Parasternal long-axis **(A)**, parasternal short-axis **(B)**, and modified apical three-chamber **(C)** imaging, demonstrating the circumscribed, heterogenous pericardial mass (M) with a cystic component (*asterisk*) adjacent to left ventricle (LV). *LA*, Left atrium.

but it is less widely available. Although TEE has excellent spatial resolution, it is nevertheless an invasive study. Tissue characterization by means of any echocardiography is limited. It is very important to understand and delineate the exact extent and depth of potential myocardial invasion from the mass. This is because myocardial invasion by the mass would potentially alter the surgical technique.

CMR can help resolve these issues. Contrast-enhanced CMR can help delineate the surface and margins of the mass, as well as any potential myocardial invasion. CMR perfusion sequences can help assess the presence and extent of vascularity of the mass, and CMR is generally accepted as the gold standard established technique in the evaluation of cardiac masses. It allows accurate confirmation of the presence of space-occupying lesions, localization and assessment of the extent of invasion, evaluation of the functional impact of the lesion, and tissue characterization. CMR is essential for diagnosis and prognosis and assists with planning of therapy, including surgical resection.

CMR is not well suited to imaging of small, highly mobile masses and can be limited by claustrophobia or contraindicated because of a history of metal fragments or some implants. Delayed enhancement imaging is also contraindicated in the setting of renal dysfunction, because of the risk for nephrogenic systemic sclerosis.

Cardiac CT with contrast may offer an alternative imaging option for mass evaluation, although it involves radiation exposure and is contraindicated in those with renal failure or contrast allergy. Combining PET with cardiac CT or CMR provides a combination of cross-sectional anatomic imaging with metabolic activity. This can be useful in evaluating disease activity to differentiate a benign from a malignant etiology and to differentiate between radiation-induced necrosis and tumor recurrence in a setting of prior surgery. FDG PET/CT was a particularly useful imaging choice for our patient, who presented with right submandibular mass, to evaluate the extent of disease spread.

CONCLUSION

We describe a rare case of a large metastatic pericardial leiomyosarcoma, with comprehensive preoperative multimodality cardiovascular imaging assessment. The combination of the strengths of both TTE and TEE provided excellent diagnostic information about the cardiac mass in our case, while both CT and CMR provided further anatomic delineation, along with valuable tissue characterization of the mass by CMR. Additionally, PET was able to provide functional assessment of the metabolic activity of the metastatic cardiac mass. It is important to use multimodality imaging to access the benefits of each modality to provide the best patient care possible with the most optimal outcomes. Multimodality imaging was essential to providing the best possible outcome for our patient.

SUPPLEMENTARY DATA

Supplementary data related to this article can be found at https://doi.org/10.1016/j.case.2018.04.007.

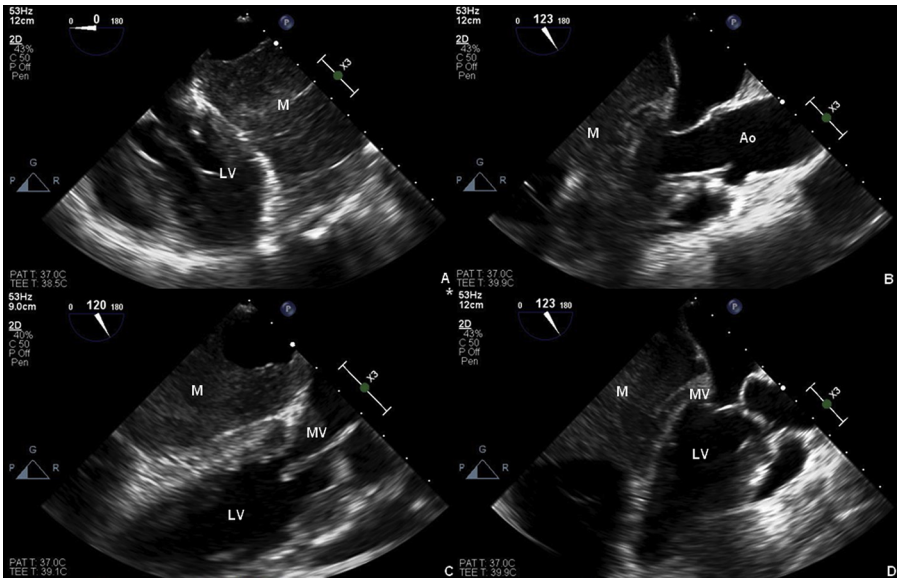

Figure 5 Transesophageal echocardiography. Midesophageal four-chamber view **(A)** and midesophageal long-axis **(B–D)** imaging, demonstrating the large heterogeneous pericardial mass (M) adjacent to the left ventricle (LV) and its relationship to the aorta (Ao). There is no apparent invasion of the myocardium. *MV*, Mitral valve.

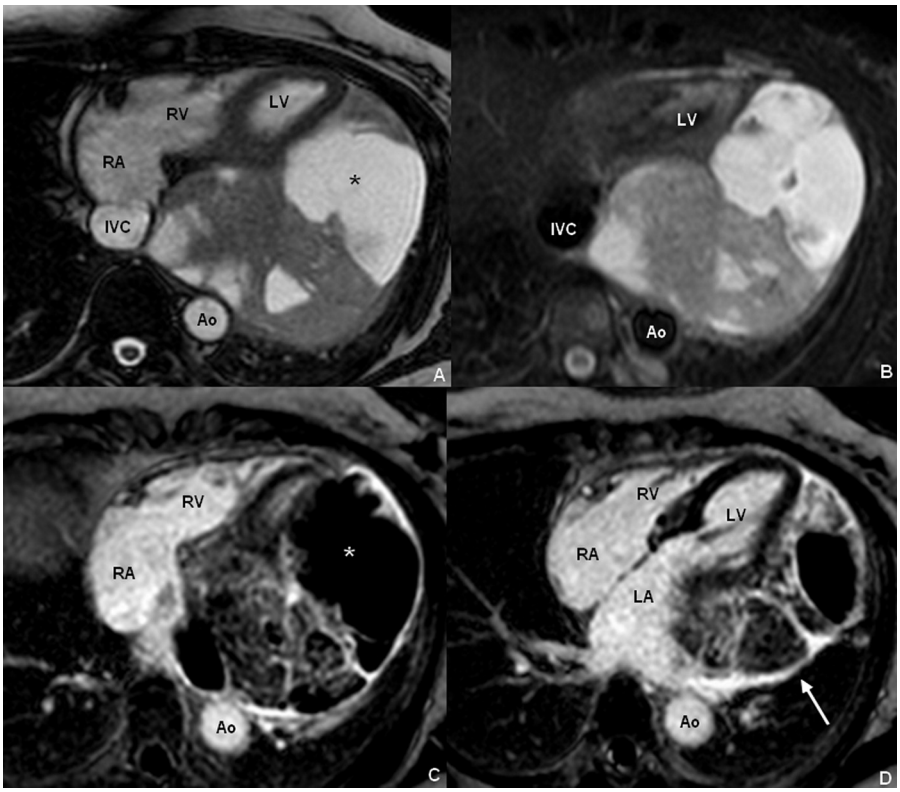

Figure 6 Cardiac magnetic resonance imaging: axial steady-state free precession **(A)** fat saturation T2-weighted short-tau inversion recovery **(B)**, and delayed enhancement imaging (phase-sensitive inversion recovery images) **(C, D)** demonstrate a large, heterogeneous mass containing multiple regions of increased signal on T1- and T2-weighted imaging, without perfusion or delayed enhancement, which are suggestive of fluid (*asterisk*). The remainder of the mass bulk has signal characteristics consistent with soft tissue. Increased signal around the lateral aspect of the mass on delayed enhancement imaging (*white arrow*) suggests fibrous encapsulation, which is not apparent adjacent to the left ventricle (LV), where tissue planes are not well defined, suggestive of epicardial invasion. *Ao*, Aorta; *IVC*, inferior vena cava; *LA*, left atrium; *RA*, right atrium; *RV*, right ventricle.

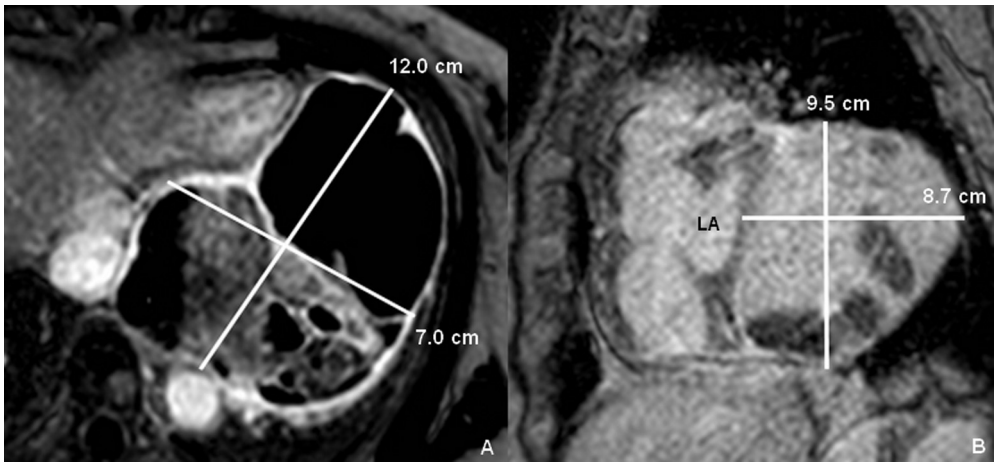

Figure 7 **(A)** Cardiac magnetic resonance imaging: axial contrast enhancement image and **(B)** sagittal contrast enhancement image demonstrating measurement of the mass, approximately 12.0 × 7.0 cm in the axial plane and 9.5 × 8.7 cm in the sagittal plane. **(B)** The left atrium (LA) is mildly compressed by the mass.

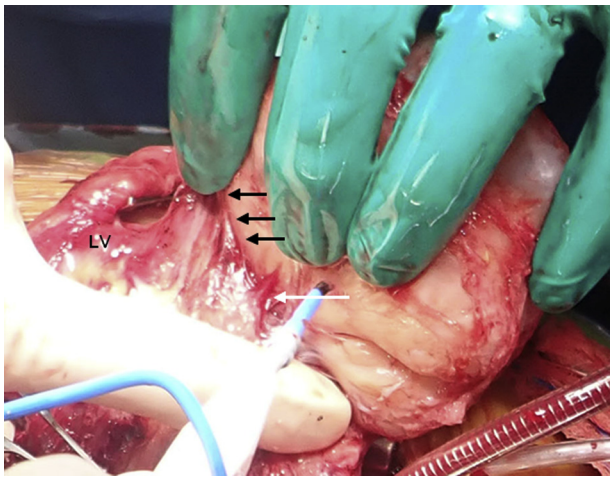

Figure 8 Intraoperative photograph, showing mass arising from a pedicle on the posterolateral aspect of the left ventricle (LV; *white arrow*), with a small amount of epicardial invasion into the posterolateral surface of the left ventricle (*black arrows*).

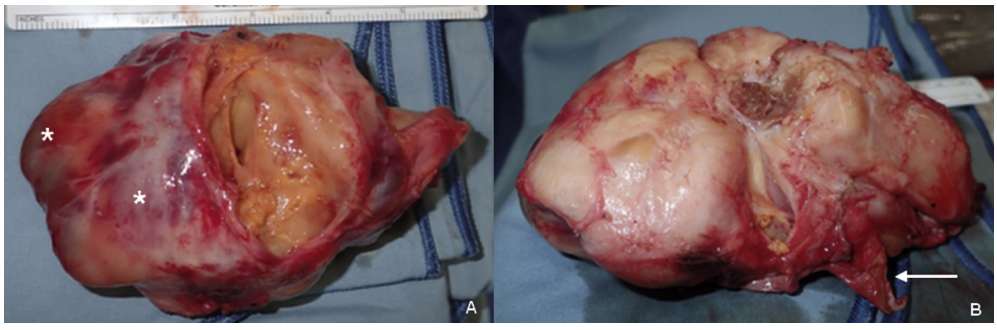

Figure 9 **(A)** Intraoperative photograph, showing a large mass with both solid and cystic components; *asterisks* highlight the cystic components of the mass. **(B)** A small amount of myocardium was resected (*white arrow*).

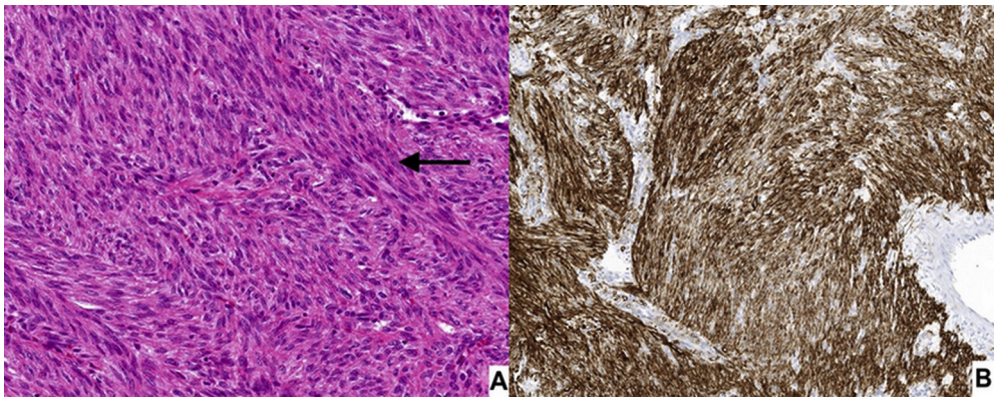

Figure 10 **(A)** Hematoxylin- and Eosin–stained section showing bundles of malignant smooth muscle cells arranged in intersecting fascicles (*black arrow*). **(B)** Desmin stain is strongly positive, supporting the diagnosis of leiomyosarcoma.

REFERENCES

1. Harlow B, Weiss N, Lofton S. The epidemiology of sarcomas of the uterus. J Natl Cancer Inst 1986;76:399-402.
2. D'Angelo E, Prat J. Uterine sarcomas: a review. Gynecol Oncol 2010;116:131-9.
3. Cheng CJ, Hong GJ, Yang SP, Tsao TP. Pulmonary metastatic leiomyosarcoma with left atrial extension via the pulmonary vein manifests as acute pulmonary edema. Acta Cardio Sin 2004;20:112.
4. Tirumami SH, Deaver P, Shinagare AB, Tirumani H, Hornick JL, George S, et al. Metastatic pattern of uterine leiomyosarcoma: retrospective analysis of the predictors and outcome in 113 patients. J Gynecol Oncol 2014;25:306-12.
5. Peng YJ, Hueng GG, Lee HS. Acute heart failure as manifestation of metastatic uterine leiomyosarcoma to the heart and lung. Heart Lung 2004;33:46-9.
6. Artioli G, Borgato L, Calamelli S, Azzarello G. Unusual cardiac metastasis of uterine leiomyosarcoma: case report and literature review. Tumori 2016;102(suppl 2):e90-2.
7. Nguyen SKA, Wong F. Right atrial metastasis of uterine leiomyosarcoma causing obstructive shock. Curr Oncol 2012;19:e292-4.
8. Katayama K, Takahashi S, Sueda T. Rupture of a metastatic uterine leiomyosarcoma invading the right atrium causing cardiac tamponade. Ann Thorac Surg 2017;104:e83.
9. Marak CP, Ponea AM, Alappana N, Shaheen S, Guddatib AK. Uterine leiomyosarcoma manifesting as a tricuspid valve mass. Case Rep Oncol 2013;6:119-26.
10. Calleja AM, Wellnitz CV, Alharthi MS, Khandheria BK, Chaliki HP. Extensive cardiac metastases secondary to uterine leiomyosarcoma. J Am Soc Echocardiogr 2009;22:1419.
11. Moreno Antón F, Casado Herraez A, Puente Vázquez J, Gómez Díaz R, Aragoncillo P, Díaz-Rubio García E. Cardiac metastasis from uterine leiomyosarcoma. Clin Transl Oncol 2006;8:375-8.
12. Karass A, Mondal P, Alkayem M, Ojo A, Aronow WS, Puccio C. A rare presentation of acute heart failure secondary to aggressive uterine leiomyosarcoma metastatic to the myocardium initially diagnosed as hypertrophic obstructive cardiomyopathy. Ann Transl Med 2016;4:374.
13. Dencker M, Valind S, Stagmo M. Right ventricular metastasis of leiomyosarcoma. Cardiovascular Ultrasound 2009;7:20.
14. Martin JL, Boak JG. Cardiac metastasis from uterine leiomyosarcoma. J Am Coll Cardiol 1983;2:383-6.
15. Zmaimita H, Samlali H, Rachdi A, Taleb A, Bouchbika Z, Benchekroune N, et al. Cardiac metastasis of uterine leiomyosarcoma: case report and literature review. Oncol Cancer Case Rep 2017;3:1.